# Soft Matter

www.rsc.org/softmatter

Volume 9 | Number 2 | 14 January 2013 | Pages 331–598

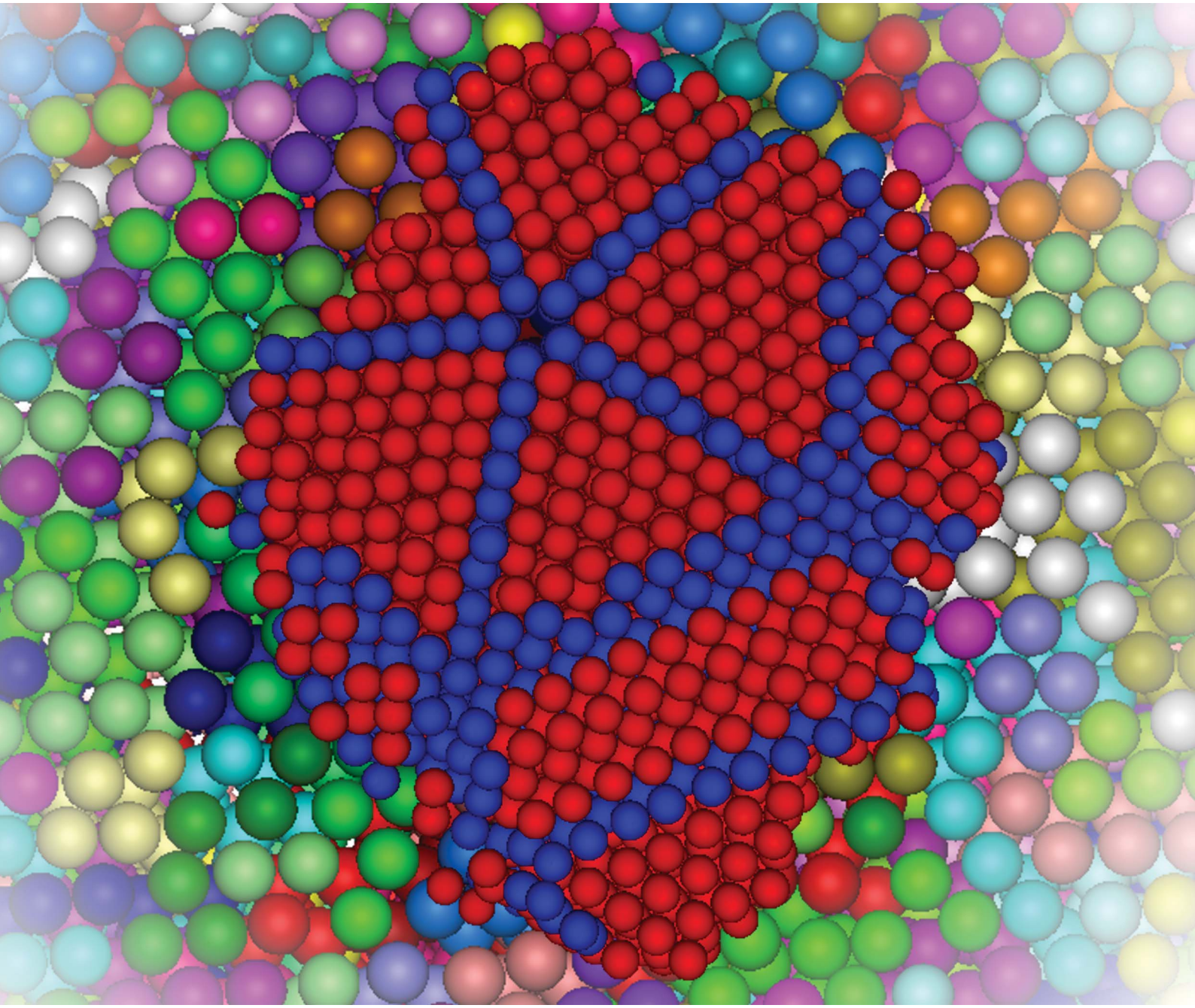

ISSN 1744-683X

RSC Publishing

**COMMUNICATION**

Ran Ni and Marjolein Dijkstra

Effect of bond length fluctuations on crystal nucleation of hard bead chains

1744-683X(2013)9:2;1-J

Soft Matter

RSC Publishing

COMMUNICATION

# Effect of bond length fluctuations on crystal nucleation of hard bead chains†

Cite this: *Soft Matter*, 2013, 9, 365

Received 24th August 2012
Accepted 15th October 2012

DOI: 10.1039/c2sm26969d

www.rsc.org/softmatter

Published on 29 October 2012 on http://pubs.rsc.org | doi:10.1039/C2SM26969D
Downloaded on 08 January 2013

Ran Ni and Marjolein Dijkstra

**We study the effect of bond length fluctuations on the nucleation rate and crystal morphology of linear and cyclic chains of flexibly connected hard spheres using extensive molecular dynamics simulations. For bond length fluctuations as small as a tenth of the bead diameter, the relaxation and crystallization resemble those of disconnected spheres. For shorter bond lengths and chains with <10 beads the nucleation rates depend sensitively on the bond length, number of beads per chain, and chain topology, while for longer chains the nucleation rates are rather independent of chain length. Surprisingly, we find a nice data collapse of the nucleation rate as a function of the number of bonds per sphere in the system, independent of bead chain composition, chain length and topology. Hence, the crystal nucleation rate of bead chains can be enhanced by adding monomers to the system. We also find that the resulting crystal morphologies of bead chains *with bond length fluctuations* resemble closely those of hard spheres including structures with a five-fold symmetry.**

Although crystal nucleation from a supersaturated fluid is one of the most fundamental processes during solidification, the mechanism is still far from being well understood. Even in a relatively simple model system of pure hard spheres, the nucleation rates obtained from Monte Carlo (MC) simulations using the umbrella sampling technique differ by more than 6 orders of magnitude from those measured in experiments.[1] This discrepancy in the nucleation rates has led to intense ongoing debates in the past decade on the reliability of various techniques employed in simulations and experiments to obtain the nucleation rates.[2,3] Recently, it was shown that the theoretical prediction of the nucleation rates for hard spheres is consistent for three widely used rare-event techniques, despite the fact that the methods treat the dynamics very differently.[3] Moreover, the structure of the resulting crystal nuclei as obtained from the different simulation techniques all agreed and showed that the nuclei consist of approximately 80% face-centered-cubic-like particles. The predominance of face-centered-cubic-like particles in the critical nuclei is unexpected, as the free energy difference between the bulk face-centered-cubic (fcc) and hexagonal-close-packed (hcp) phases is about 0.001 $k_BT$ per particle, and one would thus expect to find a random-hexagonal-close-packed (rhcp) crystal phase.[4] More surprisingly, simulation studies showed that the subsequent growth of these critical nuclei resulted in a range of crystal morphologies with a predominance of multiple twinned structures exhibiting in some cases structures with a five-fold symmetry.[5,6] Such structures are intriguing as the five-fold symmetry is incompatible with space-filling periodic crystals. Moreover, the formation mechanism of these five-fold structures is still unknown. Bagley speculated that the five-fold structures are due to the growth of five-fold local structures (a decahedral or pentagonal dipyramid cluster of spheres)[7] that are already present in the supersaturated fluid phase.[8] Another mechanism that has been proposed is that these multiple twinned structures with a five-fold symmetry originate from nucleated fcc domains that are bound together by stacking faults.[7] For instance, five tetrahedral fcc domains can form a cyclic multiple twinned structure with a pentagonal pyramid shape. A recent event-driven molecular dynamics simulation study on hard spheres showed, however, no correlation between the five-fold local clusters that are already present in the supersaturated fluid and the multiple twinned structures in the final crystal phase.[6] Hence, it was concluded that crystalline phases with multiple stacking directions may possess five-fold structures, whereas crystals with a unique stacking direction do not show any five-fold symmetry patterns. These authors also succeeded in studying the crystallization of tangent hard-sphere chains by introducing several clever (unphysical) chain-connectivity altering MC moves.[9] Surprisingly, they observed that tangent hard-sphere chains (no bond length fluctuations) never formed crystalline structures with a five-fold symmetry as the chain connectivity prohibits the formation of twinned structures and forces the crystals to grow in a single stacking direction.[6,10] Crystallization of more realistic polymer models has also been studied using computer simulations.[11–14]

*Soft Condensed Matter, Debye Institute for NanoMaterials Science, Utrecht University, Princetonplein 5 3584CC, Utrecht, The Netherlands. E-mail: r.ni@uu.nl; m.dijkstra1@uu.nl; Fax: +31 30 2532706; Tel: +31 30 2533270*

† Electronic supplementary information (ESI) available: The plot of long time diffusion coefficients of hard-sphere polymers. See DOI: 10.1039/c2sm26969d

Published on 29 October 2012 on http://pubs.rsc.org | doi:10.1039/C2SM26969D
Downloaded on 08 January 2013

In this Communication, we study the effect of bond length fluctuations on the nucleation rate and crystal morphology of flexibly connected hard spheres. These hard-sphere chains with bond length fluctuations can serve as a simple model for granular ball chains,[15] colloidal bead chains[16] or (short) polymeric systems. A better understanding of the behavior of these bead chains may shed light on the glass transition and crystallization of polymers. In fact, it has been shown recently that random packings of granular ball chains show striking similarities with the glass transition in polymers.[15] Moreover, the scaling dependence of a number of physical characteristics on packing densities at concentrations which still remain unreachable in simulations of atomistic or coarse-grained polymer models has been studied by employing this polymeric hard-sphere chain model.[17,18] We also mention that recently, a colloidal model system of bead chains has been realized consisting of colloidal spheres that are bound together with "flexible linkers".[16]

We consider a system of $M$ bead chains consisting of $N$ identical hard spheres with diameter $\sigma$ in a volume $V$. The hard-sphere beads are connected by flexible bonds with a bond energy $U_{\mathrm{bond}}(r_{ij})$ given by

$$\frac{U_{\mathrm{bond}}(r_{ij})}{k_{\mathrm{B}}T} = \begin{cases} 0 & \sigma < r_{ij} < \sigma + \delta \\ \infty & \text{otherwise} \end{cases} \quad (1)$$

where $r_{ij}$ is the center-to-center distance between the two connected spherical beads $i$ and $j$, $\delta$ is the maximum bond length, $k_{\mathrm{B}}$ is the Boltzmann constant, and $T$ is the temperature. The maximum bond length $\delta$ varies from 0 to $0.1\sigma$ in our simulations, such that $\delta = 0$ corresponds to a freely jointed chain of tangent hard spheres. We employ event driven molecular dynamics (EDMD) simulations[19,20] instead of the extensive MC method[9] to mimic the dynamics of granular and colloidal bead chains with flexible bonds. Since the pair potentials between all spheres are discontinuous, the pair interactions only change when the beads collide or when the maximum bond length is reached. Hence, the particles move in straight lines (ballistically) until they encounter another particle or reach the maximum bond length. The particles then perform an elastic collision. These collisions are identified and handled in the order of occurrence using an EDMD simulation.[21]

We study the effect of bond length fluctuations on the nucleation of bead chains at a packing fraction of $\eta = 0.55$, which is at the upper boundary of the nucleation regime of hard spheres. At $\eta = 0.55$, the nucleation time exceeds the relaxation time, which enables us to equilibrate the metastable fluid and to measure the nucleation rate. To initialize the system at this high packing fraction, we first generate a system containing random linear or cyclic chains of beads with diameter zero. To this end, we choose a random position for the first bead and subsequently generate a random angle and bond length, which is randomly chosen between 0 and $\delta$ for the next beads until the desired chain length is reached. The diameter of spheres is then grown by employing the Lubachevsky–Stillinger algorithm[22] with a very fast speed, *i.e.*, $\mathrm{d}\sigma(t)/\mathrm{d}t = 0.01\sigma/\tau$ where $\sigma(t)$ is the size of spheres at time $t$ with $\sigma$ the target sphere size and $\tau = \sigma\sqrt{m/k_{\mathrm{B}}T}$ the MD time scale. We monitor the relaxation of the initial configurations by comparing the bond angle distributions with those of previous work[23] and by calculating the long-time self-diffusion coefficient $D_{\mathrm{L}}$ of the beads. We find that $D_{\mathrm{L}}$ increases linearly with $1/N$ as predicted by the Rouse model,[24] and is rather independent of the bond length $\delta$, at least for the range of values that we studied.[25] In order to exclude the effect of dynamics on the nucleation rates,[3,26] we use the long-time diffusion coefficient of the beads, $\tau_{\mathrm{L}} = \sigma^2/6D_{\mathrm{L}}$, as the unit of time in the nucleation rate. Starting from the metastable fluid phase, an EDMD simulation is employed to evolve the system until a spontaneous nucleation event occurs. The nucleation rate is then given by $I = 1/\langle t\rangle V$, where $\langle t\rangle$ is the average waiting time before a nucleation event occurs in a system of volume $V$. In order to identify the crystalline clusters in the fluid phase, we employ the local bond-order parameter analysis.[26,27]

We calculate the crystal nucleation rates in systems consisting of $10^4$ beads for various linear and ring-like hard-sphere polymers of chain length $1 \le N \le 20$ and various bond lengths $\delta$. We mention here that we did not exclude inter-ring catenations in the configurations of ring polymers, which may occur for rings with $N \ge 5$. Fig. 1 shows that for $\delta$ as small as $0.1\sigma$, the nucleation rate resembles that of loose hard spheres. For $\delta < 0.1\sigma$, we find that the nucleation rate decreases by several orders of magnitude with decreasing $\delta$ and increasing chain length $N$, but remains constant for sufficiently long polymers, *i.e.*, $N \ge 10$. To check this surprising result, we also determined the nucleation rate of a single polymer of length $N = 10^4$ and $\delta = 0.05\sigma$, where all the beads are doubly connected except the two end beads. We observed that the system remains in the fluid phase for $7000\tau$ before a critical nucleus of $\sim$100 beads forms in the middle of the chain, which subsequently grows further until the whole system is crystalline. In Fig. 2, we show the size of the largest crystalline cluster as a function of simulation time from a typical MD trajectory. Additionally, we find that the nucleation rate does not decrease significantly for $N = 10^4$, which is highly unexpected as the beads can only move collectively.

Additionally, we did not observe spontaneous nucleation within our simulation times for linear bead chains with $\delta = 0.04\sigma$ and $N > 5$, which is to be expected as the bead chains become too frustrated on an fcc lattice at $\eta = 0.55$. At this density, the lattice spacing is

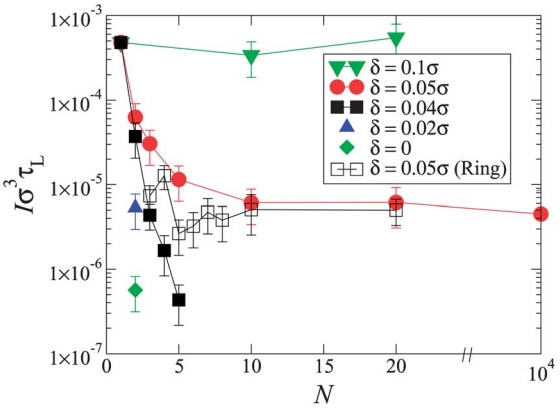


**Fig. 1** Nucleation rates $I\sigma^3\tau_{\mathrm{L}}$ of linear hard-sphere polymers with maximum bond lengths $\delta = 0.1\sigma$ (green triangles), $0.05\sigma$ (solid circles), $0.04\sigma$ (solid squares), and of ring-like hard-sphere polymers with maximum bond length $\delta = 0.05\sigma$ and chain length (open squares). For comparison, we also plot the nucleation rate for hard dumbbells with maximum bond lengths $\delta = 0.02\sigma$ (blue triangles) and $\delta = 0$ (diamonds). The error bar is the standard error of the obtained nucleation rates from independent simulations.


This journal is © The Royal Society of Chemistry 2013

Published on 29 October 2012 on http://pubs.rsc.org | doi:10.1039/C2SM26969D
Downloaded on 08 January 2013

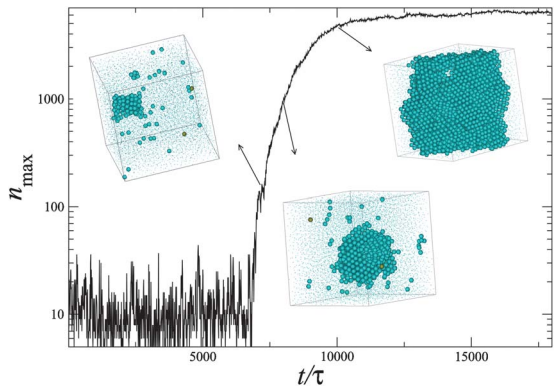


**Fig. 2** Size of the largest crystalline cluster $n_{max}$ as a function of simulation time for a single linear hard-sphere polymer with chain length $N = 10^4$. The insets are snapshots at $t = 7060\tau$, $8000\tau$ and $10\,000\tau$, respectively, where only the solid-like beads are shown, and the two dark yellow spheres are the two ends of the chain.

much larger than the sum of maximum bond length and bead diameter and thus the nucleation is strongly inhibited by lattice frustration. However, for higher packing fraction (lattice spacing similar to $\delta + \sigma$), the nucleation barrier vanishes at such a high supersaturation and crystallization sets in immediately: the nucleation rate is undefined here. For lower $\eta$, the nucleation times for bead chains exceed rapidly our simulation times, and again the rate cannot be determined. Finally, we also determine the nucleation rates for cyclic bead-chains (ring polymers) with bond length $\delta = 0.05\sigma$. Fig. 1 shows that the nucleation rate of ring polymers does not decrease monotonically with $N$ and is always lower than that of linear polymers with the same length. However, the difference in the nucleation rate is small for $N \geq 10$.

As mentioned above, our results show that the nucleation rates of linear polymers decrease with chain length $N$. One may argue that the nucleation rate is largely determined by the chain connectivity or the average number of bonds per sphere in the system. In Fig. 3, we plot the nucleation rate for linear bead chains with maximum bond length $\delta = 0.04\sigma$ and chain length $N = 1$, 2, 3, 4, and 5, which correspond to an average number of bonds per bead of $n_b = (N-1)/N = 0$, 1/2, 2/3, 3/4 and 4/5. In order to investigate the effect of average number of bonds per bead in the system on the nucleation rate, we also perform simulations for binary mixtures of linear and ring polymers with different chain lengths and bond length $\delta = 0.04\sigma$. We consider mixtures of linear chains with lengths $N = 2$ and 5, $N = 1$ and 6, and $N = 1$ and 10, and a mixture of monomers and ring polymers with $N = 10$ and 20. The composition of the mixture is chosen such that the value of $n_b$ matches with one of the values for the pure systems. We compared the nucleation rates for the pure and binary systems in Fig. 3, and observed a nice data collapse, suggesting that the nucleation rate is determined by the number of bonds per sphere in the system, and the frustration imposed by the chain connectivity in these systems. We wish to remark here that no nucleation was observed in pure systems of linear or ring polymers with $\delta = 0.04\sigma$ and $N \geq 10$ within our simulation times. Thus the addition of monomers enhances significantly the nucleation of polymers.

Additionally, we investigate the structure of the resulting critical nuclei and the full-grown crystals by calculating the averaged local bond order parameters $\bar{q}_4$ and $\bar{w}_4$ for each sphere $i$ that has $N_b(i) \geq 10$ neighbours, where the two spheres are regarded as neighbours when the center-to-center distance is smaller than $r_c = 1.3\sigma$. This analysis allows us to check whether a bead is fcc-like or hcp-like.[26,28] We find that the critical nuclei contain more fcc-like than hcp-like particles, which is very similar to the critical nuclei observed in hard-sphere[3] and hard-dumbbell nucleation.[26] In addition, we find that the full-grown crystals display a range of crystal morphologies including random-stacked hexagonal close-packed crystals and structures with a five-fold symmetry pattern for all polymer systems that we considered, even for ring-like polymers with chain length as small as $N = 3$, which were not observed in the crystal of freely jointed chains of tangent hard spheres.[6] Exemplarily, Fig. 4 shows typical configurations of these five-fold symmetry patterns formed by linear hard-sphere chains of length $N = 20$ and $\delta = 0.05\sigma$, and cyclic bead chains of $N = 3$ and 5 and $\delta = 0.05\sigma$. We note that the crystal structures resemble closely those observed in MD simulations of hard spheres.[5,6] The crystal morphology is mainly determined by the crystallization kinetics rather than the bulk and surface contributions to the free energy of the nucleus. Thus, it is tempting to speculate that the crystallization dynamics of hard bead

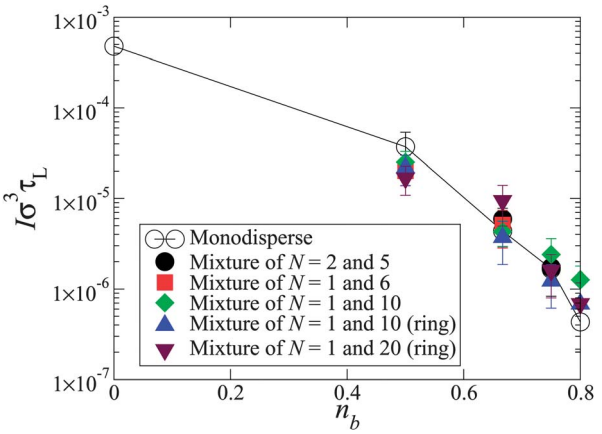


**Fig. 3** Nucleation rates $I\sigma^3\tau_L$ of linear hard-sphere polymers with chain lengths $N = 1$, 2, 3, and 5 and of binary mixtures of linear hard-sphere polymers with chain lengths $N = 2$ and 5, $N = 1$ and 6, and $N = 1$ and 10 as a function of the average number of bonds per bead $n_b$. The composition of the mixture was chosen such that the value of $n_b$ matches with one of the values for the pure systems. The maximum bond length equals $\delta = 0.04\sigma$ for all bead chains.

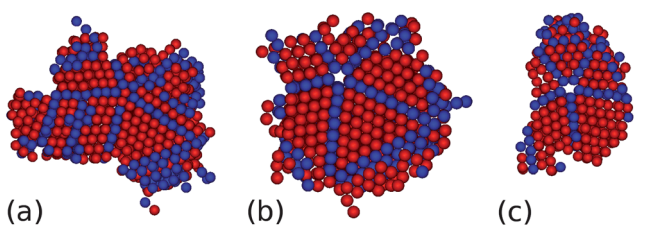


**Fig. 4** Typical configurations of the crystal structures for linear hard-sphere chains with chain length $N = 20$ (a) and for ring-like polymers with $N = 3$ (b) and $N = 5$ (c). Only crystalline spheres are shown here. The blue and red spheres are hcp-like and fcc-like particles, respectively.

Published on 29 October 2012 on http://pubs.rsc.org | doi:10.1039/C2SM26969D
Downloaded on 08 January 2013

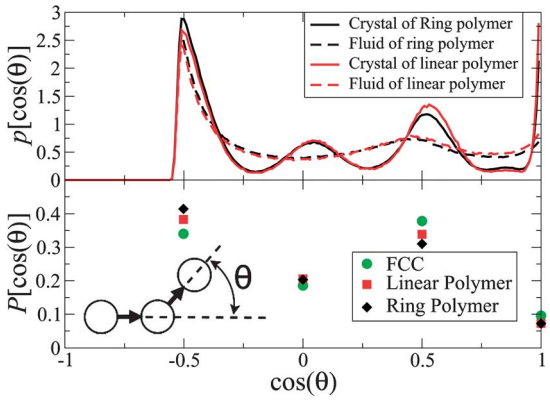


**Fig. 5** Bond angle distribution function $p(\cos\theta)$ for a supersaturated fluid and crystal of linear and cyclic hard-sphere polymers with chain length $N = 10$ and $\delta = 0.05\sigma$ (top). Integration of the peaks of $p(\cos\theta)$ between the two neighboring local minima (bottom). For comparison, we also plot the bond angle distribution for self-avoiding random walks consisting of 10 steps on an fcc crystal lattice (bottom). The inset shows the definition of the angle $\theta$.

chains *with bond length fluctuations* is similar to that of hard spheres. And it has been reported that the crystallization dynamics of hard spheres is different from tangent hard-sphere chains, which crystallize into stacking faulted layered crystals with unique stacking directions and no five-fold symmetry patterns.[10,23]

Furthermore, we determine the bond angle distribution function $p(\cos\theta)$ in order to quantify the distribution of bond angles between the two neighboring polymer bonds in the supersaturated fluid and crystal nuclei. Fig. 5 shows $p(\cos\theta)$ for systems consisting of linear and cyclic bead chains with $N = 10$. For the fluid phase, $p(\cos\theta)$ displays two peaks at $\cos\theta = -0.5$ and 0.5, *i.e.*, $\theta = 120$ and 60 degrees, which corresponds to the most frequent three particle structures observed in random packings of spheres.[23] However, $p(\cos\theta)$ of the crystal structures exhibits four pronounced peaks located around $\cos\theta = -0.5$, 0, 0.5, and 1.0 and a smaller peak at $\cos\theta = \sqrt{3}/2$, which corresponds to $\theta = 120$, 90, 60, 0 and 30 degrees, respectively.[23] In order to compare $p(\cos\theta)$ with that of a self-avoiding random walk on an fcc crystal lattice, we integrate the four pronounced peaks of $p(\cos\theta)$ between the two neighboring local minima. The results are shown in Fig. 5 together with the bond angle distribution function for a self-avoiding random walk on an fcc crystal lattice. We find that $p(\cos\theta)$ for crystals of linear and cyclic polymers agree well with that of a self-avoiding random walk.[10] Hence, $p(\cos\theta)$ seems not to be affected by the chain connectivity of the polymer chains. Free energy calculations show indeed that the stable solid of freely jointed hard-sphere chains is an aperiodic crystal phase, where the spheres are positioned on an fcc lattice with the bonds randomly oriented.[29]

In conclusion, we studied the effect of bond length fluctuations on the nucleation rate and crystal morphology of linear and cyclic hard-sphere chains by varying the maximum bond length parameter $\delta$. For sufficiently large $\delta$, *i.e.* $\sim 0.1\sigma$, the relaxation and crystallization resemble those of disconnected spheres. Hence, we find that nucleation rates and crystal morphologies are similar to those observed for hard spheres. For bond length values $0 < \delta < 0.1\sigma$, our results show on the one hand that the nucleation rates decrease significantly with $\delta$, but on the other hand the crystal morphologies of bead chains with floppy bonds resemble closely those of loose hard spheres.[5,6] Apparently, the bond constraints slow down the relaxation dynamics as the crystallization is frustrated by the chain connectivity, but do not alter the crystallization kinetics. We thus find that the resulting crystal nuclei of bead chains with bond length fluctuations possess a range of crystal morphologies including structures with a five-fold symmetry similar to hard-sphere crystals, while tangent hard-sphere chains (no bond length fluctuations) crystallize into stacking faulted layered crystals with unique stacking directions and no five-fold symmetry patterns.[10,23] Hence, the crystallization kinetic pathways of bead chains depend strongly on bond length fluctuations. Additionally, we find a nice data collapse of the nucleation rate as a function of the number of bonds per sphere in the system, independent of bead chain composition, chain length and topology. The crystal nucleation rate can thus be enhanced by the addition of monomers.

Financial support of a VICI grant from the Nederlandse Organisatie voor Wetenschappelijk Onderzoek (NWO) is acknowledged.

## References

1 S. Auer and D. Frenkel, *Nature*, 2001, **409**, 1020.
2 T. Kawasaki and H. Tanaka, *Proc. Natl. Acad. Sci. U. S. A.*, 2010, **107**, 14036.
3 L. Filion, M. Hermes, R. Ni and M. Dijkstra, *J. Chem. Phys.*, 2010, **133**, 244115.
4 P. Bolhuis, D. Frenkel, S. Mau and D. Huse, *Nature*, 1997, **388**, 235.
5 B. O'Malley and I. Snook, *Phys. Rev. Lett.*, 2003, **90**, 085702.
6 N. C. Karayiannis, R. Malshe, M. Kröger, J. de Pablo and M. Laso, *Soft Matter*, 2012, **8**, 844.
7 A. Anikeenko, N. Medvedev, A. Bezrukov and D. Stoyan, *J. Non-Cryst. Solids*, 2007, **353**, 3545.
8 B. Bagley, *J. Cryst. Growth*, 1970, **6**, 323.
9 N. Karayiannis and M. Laso, *Macromolecules*, 2008, **41**, 1537.
10 N. C. Karayiannis, K. Foteinopoulou and M. Laso, *Phys. Rev. Lett.*, 2009, **103**, 045703.
11 T. Vettorel and H. Meyer, *J. Chem. Theory Comput.*, 2006, **2**, 616.
12 T. Vettorel, H. Meyer, J. Baschnagel and M. Fuchs, *Phys. Rev. E: Stat., Nonlinear, Soft Matter Phys.*, 2007, **75**, 041801.
13 H. Meyer and F. Muller-Plathe, *Macromolecules*, 2002, **35**, 1241.
14 H. Meyer and F. Muller-Plathe, *J. Chem. Phys.*, 2001, **115**, 7807.
15 L.-N. Zou, X. Cheng, M. Rivers, H. Jaeger and S. Nagel, *Science*, 2009, **326**, 408.
16 H. R. Vutukuri, A. F. Demirörs, B. Peng, P. D. J. van Oostrum, A. Imhof and A. van Blaaderen, 2011, to be published.
17 K. Foteinopoulou, N. C. Karayiannis, M. Laso, M. Kröger and M. L. Mansfield, *Phys. Rev. Lett.*, 2008, **101**, 265702.
18 M. Laso, N. Karayiannis, K. Foteinopoulou, M. Mansfield and M. Kröger, *Soft Matter*, 2009, **5**, 1762–1770.
19 D. Rapaport, *J. Phys. A: Math. Gen.*, 1978, **11**, L213.
20 C. Hartmann, C. Schütte, G. Kalibaeva, M. D. Pierro and G. Ciccotti, *J. Chem. Phys.*, 2009, **130**, 144101.

 This journal is © The Royal Society of Chemistry 2013

21 D. C. Rapaport, *The Art of Molecular Dynamics Simulation*, Cambridge University Press, 2004.
22 B. D. Lubachevsky and F. H. Stillinger, *J. Stat. Phys.*, 1990, **60**, 561.
23 N. C. Karayiannis, K. Foteinopoulou, C. F. Abrams and M. Laso, *Soft Matter*, 2010, **6**, 2160.
24 M. Doi and S. Edwards, *The Theory of Polymer Dynamics*, Oxford University Press, 1986.
25 See ESI† for the plot of long time diffusion coefficients of hard-sphere polymers.
26 R. Ni and M. Dijkstra, *J. Chem. Phys.*, 2011, **134**, 034501.
27 P. J. Steinhardt, D. R. Nelson and M. Ronchetti, *Phys. Rev. B: Condens. Matter Mater. Phys.*, 1983, **28**, 784.
28 W. Lechner and C. Dellago, *J. Chem. Phys.*, 2008, **128**, 114707.
29 A. Malanoski and P. Monson, *J. Chem. Phys.*, 1997, **107**, 6899.

Published on 29 October 2012 on http://pubs.rsc.org | doi:10.1039/C2SM26969D
Downloaded on 08 January 2013